Zeng, L., Zielinska, H. A., Arshad, A., Hamilton-Shield, J. P., Bahl, A., Holly, J. M. P., & Perks, C. M. (2015). Hyperglycaemia-induced chemo-resistance in breast cancer cells: role of the estrogen receptor. Endocrine-Related Cancer, 125-134. [DOI: 10.1530/ERC-15-0507]. DOI: 10.1530/ERC-15-0507

Hyperglycaemia-induced chemo-resistance in breast cancer cells: role of the estrogen receptor.

*Zeng, L, *Zielinska HA, Arshad A, Shield JP, Bahl A[1], Holly JMP & Perks CM

IGFs & Metabolic Endocrinology Group, School of Clinical Sciences, University of Bristol, Learning and Research Building, Southmead Hospital, Bristol BS10 1TD. [1]Department of Clinical Oncology, Bristol Haematology and Oncology Centre, University Hospitals Bristol, Bristol, UK.

*Co-first authors

Corresponding Author: Claire M Perks

Address: IGF & Metabolic Endocrinology group, School of Clinical Sciences, University of Bristol, Learning and Research Building, Southmead Hospital, Bristol BS10 1TD

E-mail Address: claire.m.perks@bristol.ac.uk

Short Title: ERα:role in hyperglycaemia-induced chemoresistance

Keywords: Breast cancer, estrogen receptor, hyperglycaemia, chemo-resistance

Word count: 3363

Abstract

Breast cancer patients with diabetes respond less well to chemotherapy; in keeping with this we determined previously that hyperglycaemia induced chemo-resistance in estrogen receptor (ERα) positive breast cancer cells and showed that this was mediated by fatty acid synthase (FASN). More recent evidence suggests that the effect of metabolic syndrome and diabetes is not the same for all subtypes of breast cancer with inferior disease-free survival and worse overall survival only found in women with ERα positive breast cancer and not for other subtypes. Here we examined the impact of hyperglycaemia on ERα negative breast cancer cells and further investigated the mechanism underlying chemo-resistance in ERα with a view to identifying strategies to alleviate hyperglycaemia-induced chemo-resistance. We found that hyperglycaemia-induced chemo-resistance was only observed in ERα breast cancer cells and was dependent upon the expression of ERα as chemo-resistance was negated when the ERα was silenced. Hyperglycaemia induced an increase in activation and nuclear localisation of the ERα that was downstream of FASN and dependent on the activation of mitogen activated protein kinase (MAPK). We found that Fulvestrant successfully negated the hyperglycaemia-induced chemo-resistance, whereas Tamoxifen had no effect. In summary our data suggests that the ERα may be a predictive marker of poor response to chemotherapy in breast cancer patients with diabetes. It further indicates that anti-estrogens could be an effective adjuvant to chemotherapy in such patients and indicates the importance for the personalised management of breast cancer patients with diabetes highlighting the need for clinical trials of tailored chemotherapy for diabetic patients diagnosed with ERα positive breast cancers.

Introduction

Breast cancer is the most common malignancy in women with a lifetime risk of 1 in 8. In all Western societies women who present with breast cancer are increasingly likely to also suffer from co-morbid conditions such as diabetes and obesity due to the increasingly high prevalence of these conditions in the general population. In a study of over a thousand women treated for breast cancer at MD Anderson Cancer Centre in Houston, 30% were found to be obese and a further 32% overweight (Litton, et al. 2008). In addition the prevalence of metabolic syndrome in patients with breast cancer has been reported to be between 39-50% (Healy, et al. 2010; Stebbing, et al. 2012).

For all cancers, the co-morbidity of type 2 diabetes has been reported to be associated with poor prognosis and reduced survival: with a mean survival period of 10.4 years for those with diabetes and 14.3 years for those without (Currie, et al. 2012). In women with breast cancer, having metabolic syndrome was also associated with more aggressive tumour characteristics (Healy et al. 2010) and being obese confers worse overall survival (Litton et al. 2008).

Evidence also suggests that the effect of metabolic syndrome and diabetes is not the same for all subtypes of breast cancer. In a study of women involved in three large trials, inferior disease-free survival and worse overall survival was only identified in women with estrogen receptor (ERα) positive breast cancer and not for other subtypes (Sparano, et al. 2012). A recent study found that hyperglycaemia was the only feature associated with metabolic syndrome that was associated with disease progression following chemotherapy in a cohort of women with breast cancer (73% of whom had ERα positive tumors) (Stebbing et al. 2012).

In an attempt to identify the mechanisms underlying these in vivo clinical observations we previously investigated the impact of raised glucose levels on chemo-sensitivity of ERα positive breast cancer cells. We found that hyperglycaemia induced chemo-resistance in these cells, but not in non-malignant breast epithelial cells, and showed that this was mediated by increased

activity of the enzyme fatty acid synthase(FASN) which synthesises fatty acids (with glucose as the main substrate) (Zeng, et al. 2010). In keeping with the current clinical data (Stebbing et al. 2012), we found that hyperglycaemia-induced chemo-resistance was observed in ERα positive but not in ERα negative breast cancer cells. We further determined that a functional ERα was required to mediate the hyperglycaemia-induced chemo-resistance and finally that anti-estrogens may be an effective adjuvant to chemotherapy in breast cancer patients with diabetes.

Materials and Methods

Reagents and antibodies

All chemicals were purchased from Sigma (Poole, Dorset, UK). All siRNAs and the transfection reagent, HiPerFect were purchased from Qiagen (Crawley, W. Sussex, UK).

Cell Culture

The human breast cancer cell lines MCF7, T47D, MDA-MB-231 and Hs578T were purchased from ATCC that authenticates using short tandem repeat (STR) DNA profiles and the cells were used for a maximum of 10 passages. They were maintained as described before (McIntosh, et al. 2010; Zeng et al. 2010).

Dosing protocols

Cells were seeded in normal (5mM) glucose-containing growth media for 24 hours and then switched to either high (25mM) a or normal (5mM) glucose-containing serum free media for a further 48 hours with or without a MAPK inhibitor, UO126 (30μm) or for 24 hours prior to dosing with chemotherapy drugs doxorubicin (0-40μM), paclitaxel (0-300μM) or C2-ceramide (0-30μM) in the presence or absence of target siRNA to the ERα, fatty acid synthase (FASN) or non-silencing (ns) siRNA (as described previously (Foulstone, et al. 2013; Zeng et al. 2010)) or, Tamoxifen (1μM) or Fulvestrant (100nM). We used two siRNAs to silence both ERα and FASN: the second siRNA we used in this study for FASN is illustrated in supplementary figure 1.

Cell viability

This was determined by trypan blue dye exclusion assay as outlined before (McIntosh et al. 2010; Zeng et al. 2010). We confirmed apoptotic cell death by assessing the cleavage of poly (ADP-ribose) polymerase *(PARP)* using Western immunoblotting as described previously (Thomas, et al. 2009).

Cell Fractionation Assay

Cytoplasmic and nuclear fractions were separated with NE-PER Nuclear and Cytoplasmic Extraction Kit (Thermo Scientific, Cat#78835), following the manufacturers' instructions. Protein content of fractionated proteins and whole cell lysates were assessed using a BCA protein assay reagent kit (Pierce: Rockford, IL, USA) and then run on either 8/12% SDS-PAGE and transferred to a Hybond-C nitrocellulose membrane (GE Healthcare, Bucks,UK) as previously described (Zeng et al. 2010). Membranes were probed with p-ER(1:500), p-MAPK (1:1000), MAPK (1:500), tubulin (1:5000), lamin (1:1000), GAPDH (1:5000), β-actin (1:10000), FASN (1:1000) and ERα (1:750), PARP (1:1000), following the manufacturers' instructions. Tubulin and lamin were used as markers for identifying cytoplasmic and nuclear cell fractions respectively. Secondary antibodies conjugated to peroxidise were used: anti-mouse for p-ERα (1:1500), tubulin (1:5000), lamin (1:2000), GAPDH (1:5000), FASN (1:5000), ERα (1:1500), PARP (1:2000) and β-actin (1:10000). Chemiluminescence was detected using the Chemi-Doc-IT Imaging (UVP, Biorad) and analysed using Vision Works Analysis Software (UVP Inc., Upland, Ca, USA).

Chromatin Immunoprecipitation assay (ChIP)

ChIP was performed using the Imprint Immunoprecipitation kit (Cat# CHP1) from Sigma Aldrich as described before (Biernacka, 2013). Briefly, after DNA-protein crosslinking with formaldehyde, samples were sonicated and immunoprecipitated with a ChIP grade anti-ERα antibody (Millipore, Cat# 17-603). Anti-RNA polymerase II and mouse IgG supplied with the kit were used as positive and negative controls respectively. 5% input DNA was used for quantification. PCR (HotStarTaq Plus PCR Kit from Qiagen) was performed with purified DNA. The following primers were used for Cyclin D1 (CCND1): forward (−1039) AACAAAACCAATTAGGAACCTT, reverse (−770) ATTTCCTTCATCTTGTCCTTCT (as reported in Zheng, 2013(Zheng, et al. 2013)) After 38cycles, PCR products were detected by 2% agarose gel electrophoresis, stained with midori Green (Nippon

Genetics, # MG04) and analysed by Bio-Plex Imaging system from Bio-Rad (Serial No. 731BR01508).

3-(4,5-Dimethylthiazol-2-Yl)-2,5-Diphenyltetrazolium Bromide (MTT) ASSAY

The MTT assay was performed as described previously (Gill, et al. 1997; Perks, et al. 2003) . Briefly, cells were seeded into 96-well plates at 7500 (MCF7) or 22500 (T47D and MDA-MB-231) cells and treated with the chemotherapeutic drugs, doxorubicin, paclitaxel and ceramide for 48 hrs. Cells were incubated with 7.5mg/ml MTT solution for 3 hrs at 37°C. The reaction was stopped by the addition of 50µl stop solution (0.1M HCL+ 10% Triton-100) at room temperature for 20 minutes. The absorbance at 590nm was measured using an ELISA plate reader.

[3-(4,5-dimethylthiazol-2-yl)-5-(3-carboxymethoxyphenyl)-2-(4-sulfophenyl)-2H-tetrazolium (MTS) Assay

Cells were incubated with an MTS (2mg/ml, Promega, cat# G1118)/PMS (0.92mg/ml, Sigma P9625) solution at a ratio of 20:1 for 3 hrs at 37°C. 200µl of cell medium was used to measure the absorbance at 490nm with an ELISA plate reader. The cells remain viable for further analysis using this assay as opposed to the MTT assay and so we used the MTS assay for experiments in which we also wished to assess cell number and viability.

Statistical Analysis

Data were analysed with SPSS 12.0.1 for Windows using one-way ANOVA followed by least significant difference (LSD) post-hoc test. A statistically significant difference was considered to be present at $P< 0.05$.

Results

Hyperglycaemia-induced chemo-resistance is only observed in ERα positive breast cancer cells.

We demonstrated previously that ERα positive breast cancer cells, MCF7 and T47D, were resistant to cell death induced by chemotherapeutics (doxorubicin, paclitaxel and ceramide) when exposed to high levels of glucose (Zeng et al. 2010). With MCF7 cells Fig 1A confirms these previous data and Fig 1B also shows that the MTT assay also indicates the differential effects induced by altered levels of glucose: increasing doses of C2 reduced metabolic activity more effectively in normal compared to high glucose conditions. Using both the MTT assay and cell counting in this study we found that in contrast to the ERα positive breast cancer cells, ERα negative Hs578T (Fig 1C & D) and MDA-MB-231 (Fig 1E & Fig1F) cells exhibited no chemo-resistance following exposure to doxorubicin, paclitaxel or ceramide in high compared to normal glucose conditions. With Hs578T cells ceramide was able to induce cell death at 10 μM and not at the lower doses as demonstrated by the induction of PARP cleavage (insert Fig 1C), this confirms that any differential effects in response to ceramide in relation to the levels of glucose at the lower doses of ceramide as observed in the dose response (Fig 1C) were not related to the induction of cell death. We characterised the growth of the cells when exposed to normal and high levels of glucose and found that basal cell growth of ERα positive and negative cells was unaffected over 48 hours by changes in the levels of glucose (supplementary Fig2: A-D). Having observed chemoresistance in high glucose in the ERα positive breast cancer cells, we chose MCF-7 cells and assessed changes in glucoce uptake and expression of the key glucose transporters, GLUTs 1 and 12. We found that there was a 1.1-fold increase in glucose uptake in 25mM glucose that was associated with an increase in expression of GLUT 1 ($p<0.05$) and GLUT 12 ($p<0.05$). Clearly other glucose transporters are likely to play a role (supplementary Fig3 A-C).

Silencing the ERα alleviates chemo-resistance in hyperglycaemic conditions in ERα positive breast cancer cells.

Having observed that hyperglycaemia only induced chemo-resistance in ERα positive breast cancer cells, we next investigated if the presence of the ERα was required. With MCF7 cells, we found that in the presence of the ns siRNA, hyperglycaemic conditions reduced the ability of doxorubicin to induce cell death compared to euglycaemic conditions (from 31% to 23%; p=0.05) (Fig 2A) whereas with the ERα silenced, the hyperglycaemia-induced chemo-resistance was negated (Fig.2A). Similarly with T47D cells (Fig2B), in the presence of the ns siRNA, hyperglycaemic conditions reduced the ability of doxorubicin to increase cell death compared to euglycaemic conditions (from 24% to 18%; $p<0.05$) (Fig 2B) whereas with the ERα silenced, the hyperglycaemia-induced chemo-resistance was negated (Fig. 2B). With MCF7 and T47D cells we also showed that in the presence of the ns siRNA that high glucose reduced the ability of doxorubicin to decrease metabolic activity (from 0.43 fold to 0.26 fold and from 0.37 fold to 0.06; p=0.05: $p<0.05$ respectively) (Figs 2C & 2D) and that this was negated in each cell line when the ERα was silenced (Figs 2C & 2D respectively).

The western blot (Fig 2E) shows effective silencing of the ERα in both MCF7 and T47D cells in 5 and 25mM glucose conditions. The blot for PARP also confirms the chemo-resistant effect of high glucose by showing a clear reduction in doxorubicin-induced PARP cleavage in the ns hyperglycaemic compared to the ns euglycaemic conditions with both cell lines.

Hyperglycaemia increases phosphorylation and nuclear localization of ERα

Using cellular fractionation followed by Western blotting, we examined alterations in the localisation and phosphorylation of ERα. With MCF7 cells (Fig 3A & B), following exposure to high levels of glucose, we observed a shift in the localisation of the ERα with the ratio of ERα in cytoplasmic and nuclear part reduced from 1.9 to 0.8 ($p<0.05$). As ERα nuclear localisation is concomitant with an increase in ERα phosphorylation, we assessed changes in one of the key ERα

phosphorylation sites: ser^{118}. We observed that high levels of glucose increased total levels of ERα ser ^{118} phosphorylation and that as anticipated there was a 1.6 fold increase in ERα ser ^{118} phosphorylation in the nucleus ($p<0.01$). Similarly with T47D cells (Fig 3A & B) we observed a shift in the localisation of the ERα with the ratio of ERα in cytoplasmic and nuclear part reduced from 1.4 to 1.1 ($P<0.05$) concomitant with a 1.4 fold increase ERα ser ^{118} phosphorylation in the nucleus ($p<0.05$).

Hyperglycaemia increases nuclear ERα binding to a target gene, cyclin D1 (CCND1)

As a further confirmation of the increased nuclear localisation of the ERα, we chose to assess alterations in the association of ERα with one of its known target genes, cyclin D1, CCND1. Using ChIP assay we found that high levels of glucose caused a 2.7 fold increase ($p<0.05$) with MCF7 cells and an 11.7 fold increase ($p<0.05$) with T47D cells (Fig 3C & D) in the association of ERα with the CCND1 gene.

The hyperglycamia-induced increase in ERα ser ^{118} phosphorylation is downstream of fatty acid synthase (FASN)

We had shown previously in ERα positive breast cancer cells that hyperglycaemia-induced chemo-resistance was dependent upon FASN (Zeng et al. 2010). Having now demonstrated a role for the ERα in hyperglycaemia-induced chemo-resistance, we silenced FASN using siRNA in both MCF7 (Fig 4A) and T47D (Fig 4B) cells to determine any impact on the ERα and levels of ERα ser ^{118} phosphorylation. We found that silencing FASN reduced levels of the ERα in both normal and high glucose and reduced the ability of hyperglycaemia to activate ERα ser ^{118} phosphorylation (Fig 4C) suggesting that FASN is acting upstream of the ERα.

FASN regulates p-ERα (ser118) levels via the MAPK pathway

Having observed that the effect of hyperglycaemia on the phosphorylation of the ERα was downstream of FASN, we next wished to elucidate the mechanism through which FASN regulated p-ERα ser ^{118} levels. With MCF-7 cells, we found that in the presence of the non-silencing FASN siRNA, hyperglycaemic conditions increased p-MAPK levels (x 1.8 fold increase; p=0.01) compared to euglycaemic conditions and that this was negated when FASN was silenced (Fig 5A & B). To determine whether MAPK signalling pathway was required for the hyperglycaemia-induced increase in ERα ser ^{118} phosphorylation, we used U0126, a MAPK inhibitor. As illustrated in Fig 5C and D, treatment with U0126 completely blocked the ability of hyperglycaemia to activate ERα ser ^{118} phosphorylation. Taken together, these results indicate that FASN regulates p-ERα (ser118) levels via activation of MAPK.

Fulvestrant blocks but Tamoxifen has no effect on hyperglycaemia-induced chemo-resistance

Having shown that silencing the ERα using siRNA negated chemo-resistance induced by high glucose, we then assessed the effects of blocking the estrogen receptor in a more clinically relevant manner by using two anti-estrogens, Fulvestrant (selective estrogen receptor down regulator, SERD) and Tamoxifen (selective estrogen receptor modulator, SERM). We first ensured we were using effective doses of each of the drugs.

With fig 6A & B and Fig 7A & B we show that Fulvestrant and Tamoxifen (respectively) effectively blocked estrogen-induced ERα ser ^{118} phosphorylationin both MCF7 and T47D cell lines. We also confirmed in both cell lines that Fulvstrant down-regulates the ERα and Tamoxifen stabilises it as reported in the literature (supplementary fig 13 B&C). Having identified effective doses of both drugs we investigated if either Fulvestrant or Tamoxifen would negate hyperglycaemia-induced chemo-resistance as we had observed when the estrogen receptor was artificially silenced using siRNA. Fig 6C & 6D indicate that hyperglycaemia-induced resistance to doxorubicin-induced cell

death (18 % to 11% $p < 0.01$ and 13% to 7% respectively) was blocked by Fulvestrant in both MCF7 and T47D breast cancer cells. In contrast Fig 7C (MCF7) & D (T47D) show that Tamoxifen was ineffective in negating the hyperglycaemia-induced chemo-resistance in either cell line.

Discussion

The current report has determined that hyperglycaemia-induced chemo-resistance only occurs in breast cancer cell lines that possess a functional ERα and has identified that the ERα is key in mediating this hyperglycaemia-induced chemo-resistance. We believe that our novel data may explain important clinical observations: in a study of women involved in three large trials, inferior disease-free and overall survival was only found in women with ER positive breast cancer and not for other subtypes(Sparano et al. 2012). In addition, that hyperglycaemia was the only feature associated with metabolic syndrome that was linked with disease progression following chemotherapy in a cohort of women with breast cancer (73% of whom had ER positive tumors)(Stebbing et al. 2012). It has been reported that estrogen receptors are important regulators of components of the glycolytic pathway and contribute to the Warburg effect in cancer cells(Cai, et al. 2012). Our data indicate that the ERα is also an important determinant of how metabolic conditions specifically affect breast cancer cells and their response to chemotherapy. We clearly observed that silencing the ERα in ERα positive breast cancer cells negated hyperglycaemia-induced chemo-resistance; consistent with these findings we determined that exposing ERα negative breast cancer cells to different levels of glucose did not influence chemo-sensitivity. The ERα has been linked to chemo-resistance previously: Tokuda et al showed that silencing the ERα in MCF7 breast cancer cells enhanced sensitivity to paclitaxel (Tokuda, et al. 2012). This study was only performed under hyperglycaemic conditions and in that context their results were consistent with our findings.

As the ERα can be located at numerous sites within the cell we assessed if exposure to high glucose impacted on the localisation of the ERα. We found that hyperglycaemia increased the relative amounts of ERα in the nucleus compared to the cytoplasm. The ERα needs to be phosphorylated to translocate to the nucleus: in keeping with the ERα localisation data we observed a significant increase in phosphorylation of ERα at ser^{118}. To corroborate these findings

306 we assessed the level of ERα binding to one of its known target genes, cyclin D1 when exposed to
307 different levels of glucose: as anticipated based on the localisation and phosphorylation data, we
308 found an increase in association of the ERα with the cyclin 1 gene when ERα positive breast
309 cancer cells were exposed to high levels of glucose. Ross-Innes et al assessed the dynamics of ERα
310 binding to DNA in clinical breast cancer samples and found that differential ERα binding was
311 associated with clinical outcome in breast cancer: ERα bound to different sites and with different
312 affinities depending on the stage(Ross-Innes, et al. 2012). In light of these novel findings our data
313 may suggest that breast cancer patients with altered metabolism may have tumour cells with
314 altered ERα/DNA binding patterns that may contribute to chemo-resistance.
315 We showed previously that hyperglycaemia-induced chemo-resistance was dependent upon fatty
316 acid synthase (FASN) (Zeng et al. 2010). Associations between the ERα and FASN have been
317 identified in breast cancer cells previously (Lupu and Menendez 2006). We delineated that our
318 new data, showing the important role of the ERα, was related to our previously defined signalling
319 pathway. Our data suggests that the effect of hyperglycaemia on the phosphorylation of the ERα
320 is downstream of FASN as silencing FASN reduced activation of the ERα: in addition that the
321 increased phosphorylation of the ERα was mediated by MAPK activation downstream of FASN.
322 We then blocked the estrogen receptor in a more clinically relevant manner using two anti-
323 estrogens, Fulvestrant and Tamoxifen to assess their effectiveness in alleviating the resistance
324 induced by hyperglycaemic conditions. We found that Fulvestrant successfully negated the
325 hyperglycaemia-induced chemo-resistance, whereas Tamoxifen had no effect. We believe this
326 relates to how these two drugs act: Fulvestrant degrades the ERα whereas Tamoxifen stabilises
327 the protein. The mechanism by which Fulvestrant acts would be most comparable to our
328 experiments where we artificially silenced the ERα with siRNA.
329 In summary our data provides a mechanism to support the clinical studies indicating that women
330 with ERα positive breast cancer who also have diabetes respond less well to chemotherapy: it
331 suggests that the ERα may be a predictive marker of poor response to chemotherapy in breast

cancer patients with diabetes. It further indicates that certain classes of anti-estrogen therapy may prove effective adjuvants to chemotherapy in such patients but the specific type of anti-estrogen needs to be considered carefully. Our data indicates the potential importance and benefit of personalised medical therapy in the management of breast cancer, highlighting the need for clinical trials of tailored chemotherapy for diabetic patients diagnosed with ERα positive breast cancers.

357 **Declaration of interest, Funding and Acknowledgements**

358 The authors declare that there is no conflict of interest that could be perceived as prejudicing the
359 impartiality of the research reported. This work was supported by The European Foundation for
360 the Study of Diabetes (EFSD). HZ, LZ & AA performed the research experiments. CMP wrote the
361 manuscript, contributed to the design, obtained the funding and supervised the study. JMPH
362 contributed to the design, supervision and to the writing of the paper. AB & JS also contributed to
363 writing the paper and provided invaluable advice regarding the potential clinical applications of
364 the work. We thank Lindsay Durant for contributing to this work.

365

366

References

Cai Q, Lin T, Kamarajugadda S & Lu J 2012 Regulation of glycolysis and the Warburg effect by estrogen-related receptors. *Oncogene* **32**(16):2079-86

Currie CJ, Poole CD, Jenkins-Jones S, Gale EA, Johnson JA & Morgan CL 2012 Mortality After Incident Cancer in People With and Without Type 2 Diabetes: Impact of metformin on survival. *Diabetes Care* **35** 299-304.

Foulstone EJ, Zeng L, Perks CM & Holly JM 2013 Insulin-like growth factor binding protein 2 (IGFBP-2) promotes growth and survival of breast epithelial cells: novel regulation of the estrogen receptor. *Endocrinology* **154** 1780-1793.

Gill ZP, Perks CM, Newcomb PV & Holly JM 1997 Insulin-like growth factor-binding protein (IGFBP-3) predisposes breast cancer cells to programmed cell death in a non-IGF-dependent manner. *J Biol Chem* **272** 25602-25607.

Healy LA, Ryan AM, Carroll P, Ennis D, Crowley V, Boyle T, Kennedy MJ, Connolly E & Reynolds JV 2010 Metabolic syndrome, central obesity and insulin resistance are associated with adverse pathological features in postmenopausal breast cancer. *Clin Oncol (R Coll Radiol)* **22** 281-288.

Litton JK, Gonzalez-Angulo AM, Warneke CL, Buzdar AU, Kau SW, Bondy M, Mahabir S, Hortobagyi GN & Brewster AM 2008 Relationship between obesity and pathologic response to neoadjuvant chemotherapy among women with operable breast cancer. *J Clin Oncol* **26** 4072-4077.

Lupu R & Menendez JA 2006 Targeting fatty acid synthase in breast and endometrial cancer: An alternative to selective estrogen receptor modulators? *Endocrinology* **147** 4056-4066.

McIntosh J, Dennison G, Holly JM, Jarrett C, Frankow A, Foulstone EJ, Winters ZE & Perks CM 2010 IGFBP-3 can either inhibit or enhance EGF-mediated growth of breast epithelial cells dependent upon the presence of fibronectin. *J Biol Chem* **285** 38788-38800.

391 Perks CM, Newcomb PV, Grohmann M, Wright RJ, Mason HD & Holly JM 2003 Prolactin acts as a
392 potent survival factor against C2-ceramide-induced apoptosis in human granulosa cells. *Hum*
393 *Reprod* **18** 2672-2677.
394 Ross-Innes CS, Stark R, Teschendorff AE, Holmes KA, Ali HR, Dunning MJ, Brown GD, Gojis O, Ellis
395 IO, Green AR, et al. 2012 Differential oestrogen receptor binding is associated with clinical
396 outcome in breast cancer. *Nature* **481** 389-393.
397 Sparano JA, Wang M, Zhao F, Stearns V, Martino S, Ligibel JA, Perez EA, Saphner T, Wolff AC,
398 Sledge GW, Jr., et al. 2012 Obesity at diagnosis is associated with inferior outcomes in hormone
399 receptor-positive operable breast cancer. *Cancer* **118**(23):5937-46
400 Stebbing J, Sharma A, North B, Athersuch TJ, Zebrowski A, Pchejetski D, Coombes RC, Nicholson
401 JK & Keun HC 2012 A metabolic phenotyping approach to understanding relationships between
402 metabolic syndrome and breast tumour responses to chemotherapy. *Ann Oncol* **23** 860-866.
403 Thomas F, Patel S, Holly JM, Persad R, Bahl A & Perks CM 2009 Dihydrotestosterone sensitises
404 LNCaP cells to death induced by epigallocatechin-3-Gallate (EGCG) or an IGF-I receptor inhibitor.
405 *Prostate* **69** 219-224.
406 Tokuda E, Seino Y, Arakawa A, Saito M, Kasumi F, Hayashi S & Yamaguchi Y 2012 Estrogen
407 receptor-alpha directly regulates sensitivity to paclitaxel in neoadjuvant chemotherapy for breast
408 cancer. *Breast Cancer Res Treat* **133** 427-436.
409 Zeng L, Biernacka KM, Holly JM, Jarrett C, Morrison AA, Morgan A, Winters ZE, Foulstone EJ,
410 Shield JP & Perks CM 2010 Hyperglycaemia confers resistance to chemotherapy on breast cancer
411 cells: the role of fatty acid synthase. *Endocr Relat Cancer* **17** 539-551.
412 Zheng L, Qi T, Yang D, Qi M, Li D, Xiang X, Huang K & Tong Q 2013 microRNA-9 suppresses the
413 proliferation, invasion and metastasis of gastric cancer cells through targeting cyclin D1 and Ets1.
414 *PLoS One* **8** e55719.

415

Figure Legends

Figure 1: Hyperglycaemia-induced chemo-resistance is only observed in ERα positive breast cancer cells. **A.** Using trypan blue dye exclusion method, the percentage cell death was assessed in the ERα positive MCF7 cells treated with chemotherapeutics (Doxorubicin 1μM $p \leq 0.01$, Paclitaxel 1μM $p=0.01$ and Ceramide 12μM $p=0.01$) in 5mM and 25mM glucose for 24 hours (n=3 experiments). Changes in metabolic activity of the MCF-7 cells in 5mM and 25mM glucose in response to ceramide (0- 20μM) was examined using an MTT assay **(B)** (n=3 experiments, *: $p \leq 0.05$). The metabolic activity of the ERα negative Hs578T cells in 5mM and 25mM glucose in response to doxorubicin (DOX, 0-20μM), ceramide (C2, 0-30μM) and paclitaxel (Pac, 0-300μM) was examined with MTT assay **(C)** (n=3 experiments). Insert shows ceramide-induced PARP cleavage (85kD fragment) by Western blotting (n=3 experiments). Percentage of cell death triggered by these drugs in 5mM and 25mM glucose was assessed by trypan blue dye exclusion assay **(D)** (n=3 experiments). The change in metabolic activity of another ERα negative cell line, MDA-MB-231 in 5mM and 25mM glucose exposed to the above drugs is shown in **(E)** and percentage of cell death in **(F)** (n=3 experiments).

Figure 2: Silencing the ERα alleviates chemo-resistance in hyperglycaemic conditions in ERα positive breast cancer cells, compared to the non-silencing siRNA control (ns). Percentage of cell death induced by doxorubicin (DOX, 1μM in MCF7 and 5μM in T47D cells) was assessed in MCF7 **(A)** or T47D **(B)** cells with or without ERα knocked down with 20nM siRNA in 5 or 25mM glucose (n=3 experiments). Changes of metabolic activity induced by doxorubicin (DOX) in MCF7 **(C)** or T47D **(D)** cells were also measured with or without ERα silencing in 5 or 25mM glucose (n=3 experiments). Effective ERα knocking down and PARP cleavage was shown in **(E)**. β-actin probing was used as a loading control (n=3 experiments).

Figure 3: Hyperglycaemia increases phosphorylation and nuclear localization of ERα and increases nuclear ERα binding to a target gene, cyclin D1 (CCND1). Cell fractionation and Western blotting

were performed to examine cytoplasmic or nuclear location of ERα and p-ERα (ser^{118}) in MCF7 and T47D cells **(A)** under 5 or 25mM glucose condition. Tubulin and Lamin A/C blots were used as markers for cytoplasmic and nuclear compartments respectively (n=3 experiments,). The densitometry measurements from the western blot are shown in **(B**, $p<0.05$**)**. Chromatin Immunoprecipitation assay (ChIP) was used to examine the changes in association of the ERα with one of its target genes, cyclin D1 (CCND1) **(C)**. 5% input was used as a quantification control (n=3 experiments). The relative enrichment of the CCND1 gene bound to ERα was quantified in **(D**, $p<0.05$).

Figure 4: The hyperglycamia-induced increase in ERα (ser ^{118}) phosphorylation is downstream of fatty acid synthase (FASN). Using western blotting , the ERα and p-ERα (ser118) abundance were assessed in MCF7 **(A)** or T47D **(B)** cells, with or without fatty acid synthase (FASN) knocked down with 20nM siRNA (n=3 experiments). β-actin was probed as a loading control. Relative fold changes of p-ERα (ser^{118}) against total ERα were measured **(C**, ($p<0.05$)).

Figure 5. FASN regulates p-ERα (ser118) levels via activation of MAPK. Using western blotting, the abundance of MAPK and p-MAPK were assessed in MCF-7 cells with or without FASN silenced with 20nM siRNA in 5 or 25mM glucose (n=3 experiments) **(A)**. Relative fold changes of p-MAPK against total MAPK were measured in (**B**, $p<0.05$). Effect of MAPK inhibition with U0126 on p-Erα (ser118) was assessed in MCF-7 cells treated with or without U0126 (30μm) in 5 or 25mM glucose for 48 hours (n=3 experiments) **(C)**. The densitometry measurements from the western blot are shown in (**D**, $p<0.05$).

Figure 6: Fulvestrant blocks hyperglycaemia-induced chemo-resistance. MCF7 **(A)** and T47D **(B)** cells were treated with the anti-estrogen Fulvestrant (Ful) 100nM 24 hours prior to treatment with 10nM estrogen for 20 minutes, in 5 or 25mM glucose conditions. Western blotting was performed to show

protein abundance of ERα and p-ERα (ser^{118}). β-actin was probed as a loading control (n=3 experiments). Percentage of cell death induced by doxorubicin (DOX, 1μM in MCF7 and 5μM in T47D cells) was assessed in MCF7 **(C)** or T47D **(D)** cells with or without 24h hours pre-treatment of 100nM Fulvestrant in 5 or 25mM glucose (n=3 experiments).

Figure 7: Tamoxifen has no effect on hyperglycaemia-induced chemo-resistance. MCF7 **(A)** and T47D **(B)** cells were treated with the anti-estrogen Tamoxifen (TAM) 1μM 1 hour prior to treatment with 10nM estrogen for 20 minutes, in 5 or 25mM glucose condition. Western blotting was performed to show protein abundance of ERα and p-ERα (ser^{118}). β-actin was probed as a loading control (n=3 experiments). Percentage of cell death induced by doxorubicin (DOX) was assessed in MCF7 **(C)** or T47D **(D)** cells with or without 1 hour pre-treatment of 1μM Tamoxifen in 5 or 25mM glucose (n=3 experiments).

Supplementary Figure 1. A second siRNA sequence was used to silence FASN in MCF7 and T47D cells under 5 or 25mM glucose condition **(A) shows equivalent effective silencing of FASN** (blot representative of 3 repeats). Western blotting showing protein abundance of ERα in MCF7 and T47D cells, treated with Fulvestrant (100nM) or Tamoxifen (1μM) for 24 hours, the same time length as the exposure to the chemotherapeutics **(B)**. β-actin was probed as a loading control (n=3 experiments).

Supplementary figure 2: altered levels of glucose had no effect on basal cell growth in ERα positive or negative breast cancer cell lines. MCF7, T47D (ERα positive) and Hs578T and MDA-MB-231 (ERα negative) cells were seeded in 5 mM glucose-containing growth media for 24 hours prior to being exposed to 5mM and 25 mM-glucose containing serum free media for a further 48hrs. Total cell number was assessed by cell counting. Each experiment was repeated in triplicate and performed at least 3 times.

Supplementary Figure 3 Hyperglycaemia increases glucose uptake. Glucose uptake was assessed using tritiated 2-deoxyglucose in MCF-7 cells cultured in 5 or 25mM glucose condition for 48 hours (n=3 experiments) (**A**). Hyperglycaemia upregulates glucose transporters. The mRNA levels of GLUT1 **(B)** and GLUT12 **(C)** were quantified using SYBR green based qPCR in MCF-7 cells cultured under 5 or 25mM glucose condition for 48 hours (n=3 experiments).

Figure 1

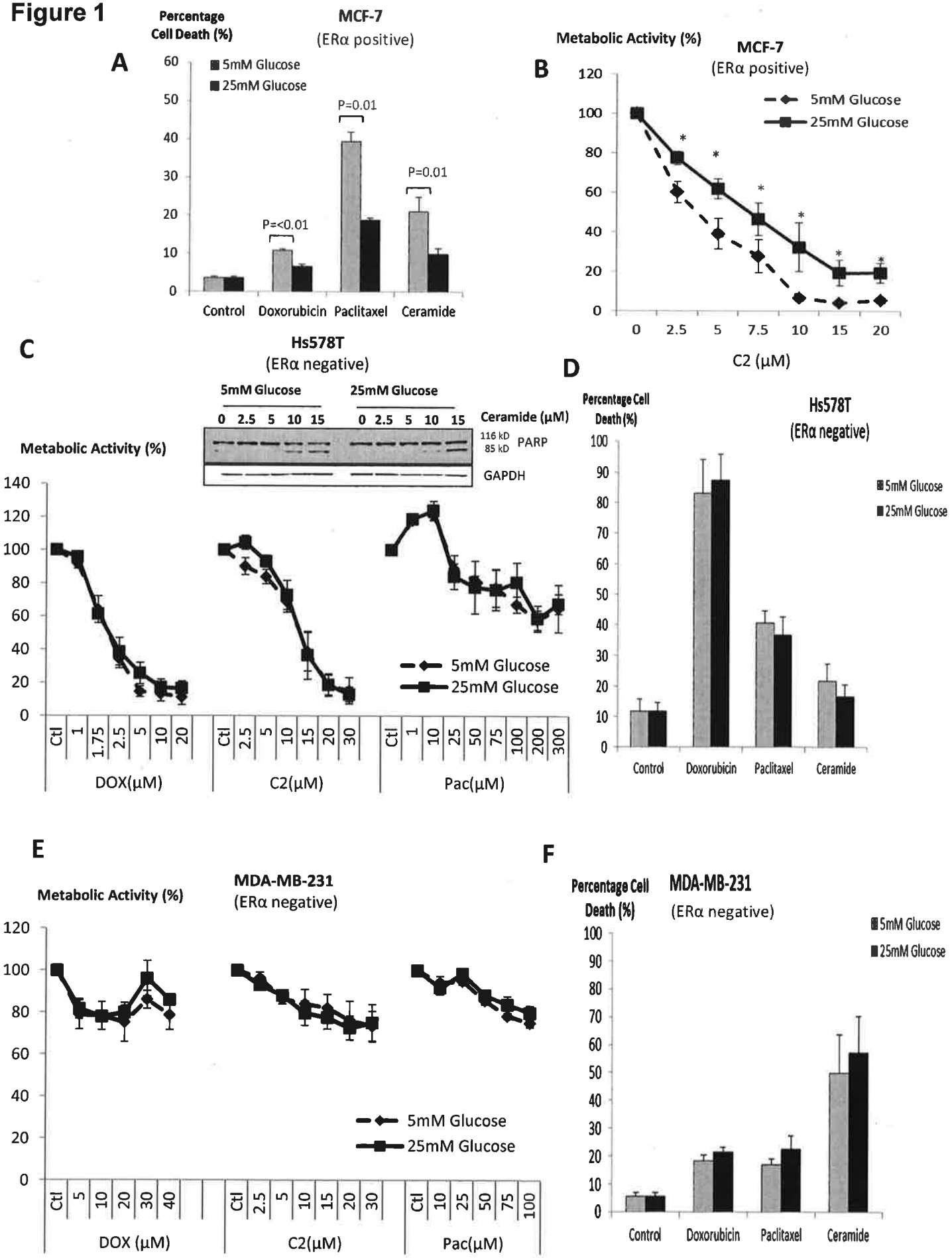
A
Percentage Cell Death (%)
MCF-7
(ERα positive)
5mM Glucose
25mM Glucose
P=0.01
P=0.01
P=<0.01
Control
Doxorubicin
Paclitaxel
Ceramide
B
Metabolic Activity (%)
MCF-7
(ERα positive)
5mM Glucose
25mM Glucose
C2 (μM)
C
Hs578T
(ERα negative)
5mM Glucose
25mM Glucose
Ceramide (μM)
116 kD
85 kD
PARP
GAPDH
Metabolic Activity (%)
DOX(μM)
C2(μM)
Pac(μM)
D
Percentage Cell Death (%)
Hs578T
(ERα negative)
5mM Glucose
25mM Glucose
Control
Doxorubicin
Paclitaxel
Ceramide
E
Metabolic Activity (%)
MDA-MB-231
(ERα negative)
5mM Glucose
25mM Glucose
DOX (μM)
C2(μM)
Pac(μM)
F
Percentage Cell Death (%)
MDA-MB-231
(ERα negative)
5mM Glucose
25mM Glucose
Control
Doxorubicin
Paclitaxel
Ceramide

Figure 2

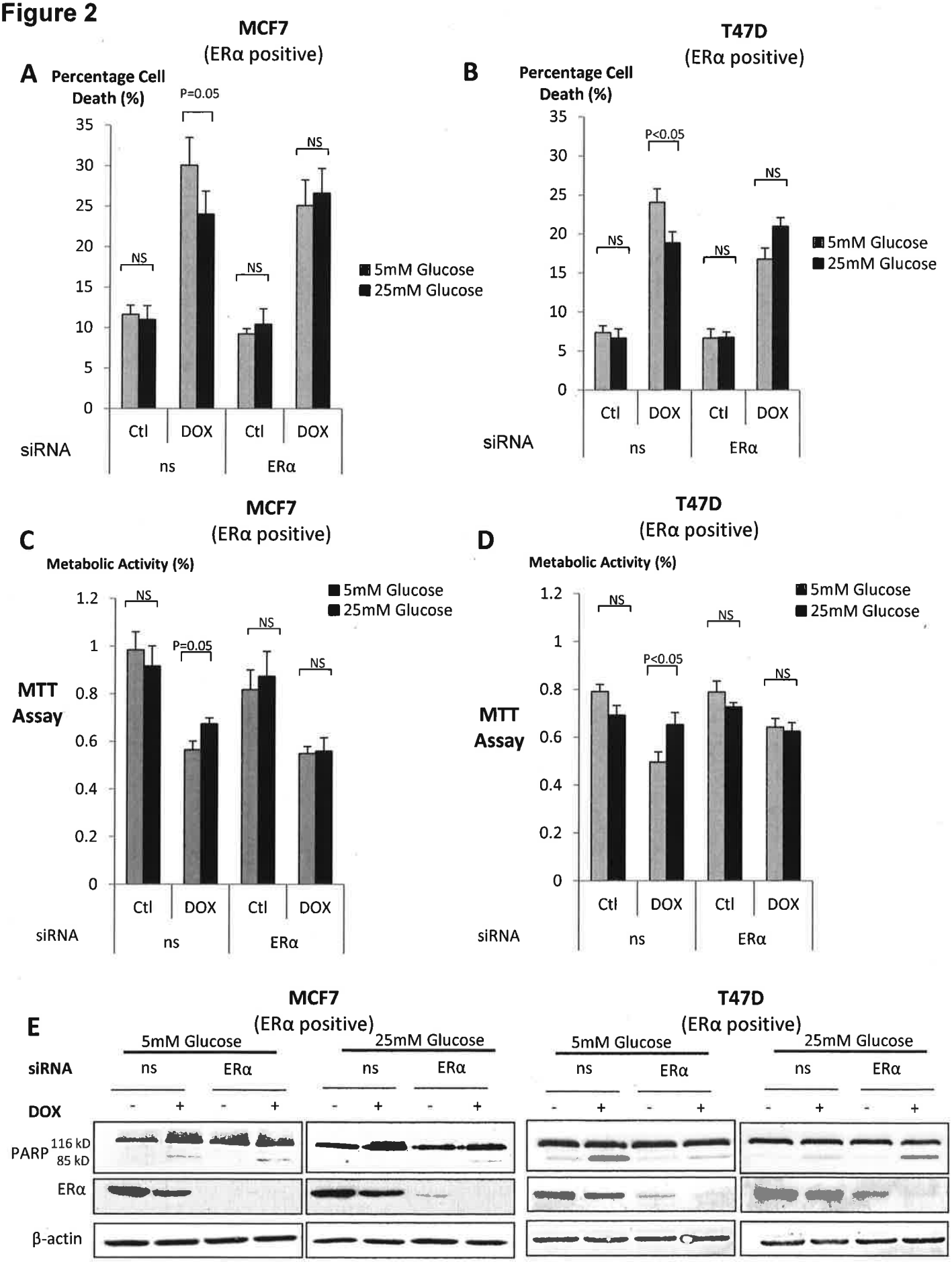
A
MCF7
(ERα positive)
Percentage Cell Death (%)
P=0.05
NS
NS
NS
5mM Glucose
25mM Glucose
Ctl
DOX
Ctl
DOX
siRNA
ns
ERα
B
T47D
(ERα positive)
Percentage Cell Death (%)
P<0.05
NS
NS
NS
5mM Glucose
25mM Glucose
Ctl
DOX
Ctl
DOX
siRNA
ns
ERα
C
MCF7
(ERα positive)
Metabolic Activity (%)
MTT Assay
P=0.05
NS
NS
NS
NS
5mM Glucose
25mM Glucose
Ctl
DOX
Ctl
DOX
siRNA
ns
ERα
D
T47D
(ERα positive)
Metabolic Activity (%)
MTT Assay
P<0.05
NS
NS
NS
NS
5mM Glucose
25mM Glucose
Ctl
DOX
Ctl
DOX
siRNA
ns
ERα
E
MCF7
(ERα positive)
T47D
(ERα positive)
5mM Glucose
25mM Glucose
5mM Glucose
25mM Glucose
siRNA
ns
ERα
ns
ERα
ns
ERα
ns
ERα
DOX
- + - + - + - + - + - + - +
PARP 116 kD
85 kD
ERα
β-actin

Figure 3

A

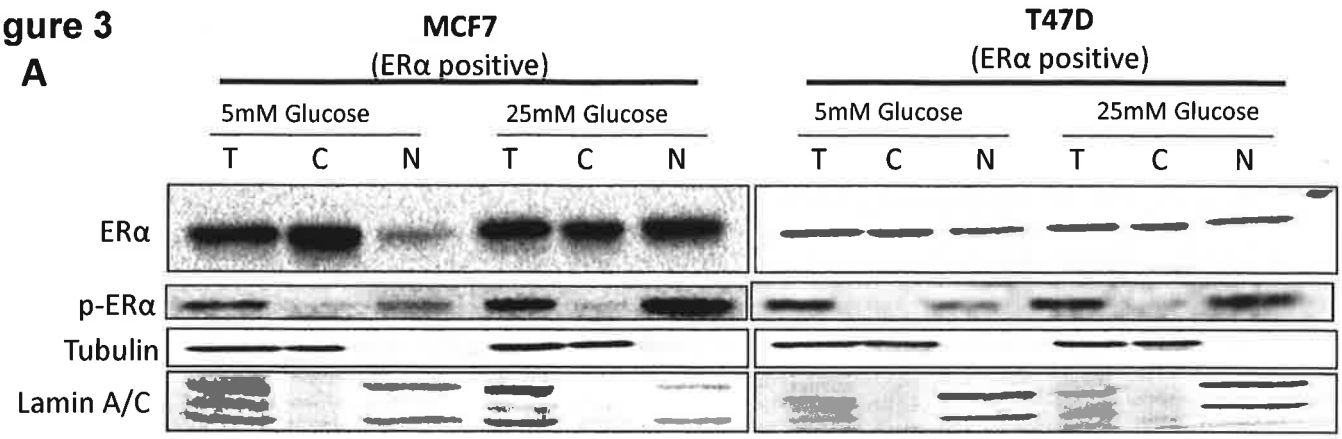

B

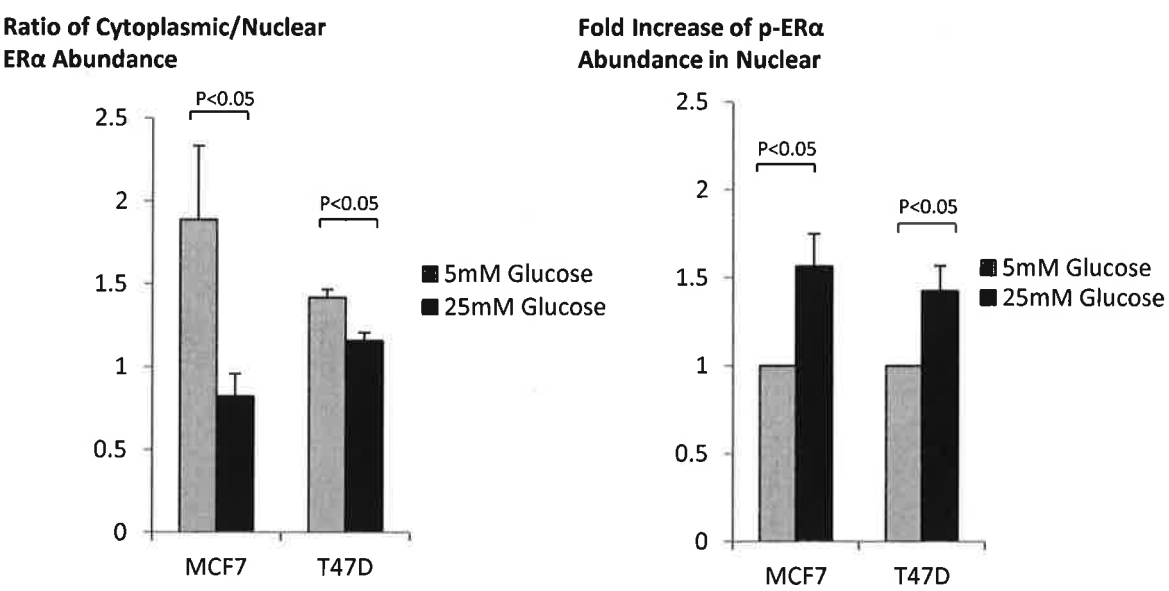

C

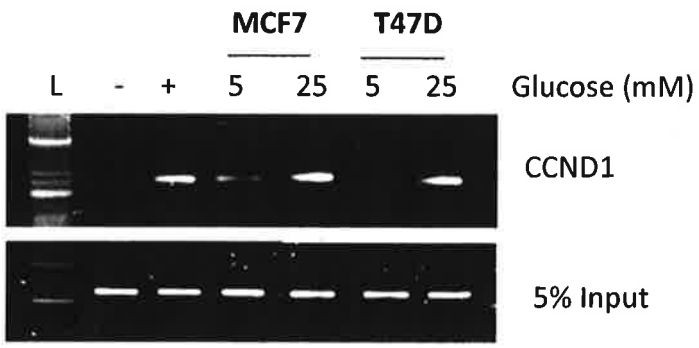

D

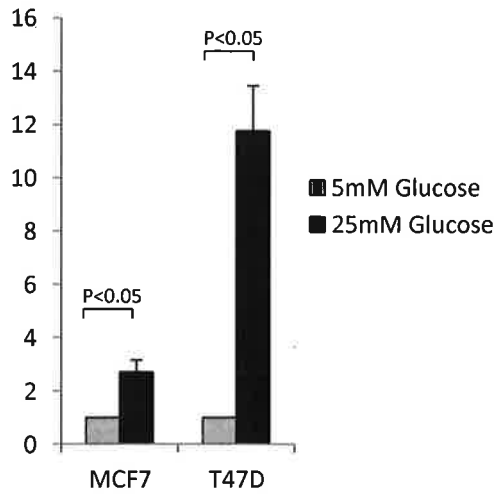

Figure 4

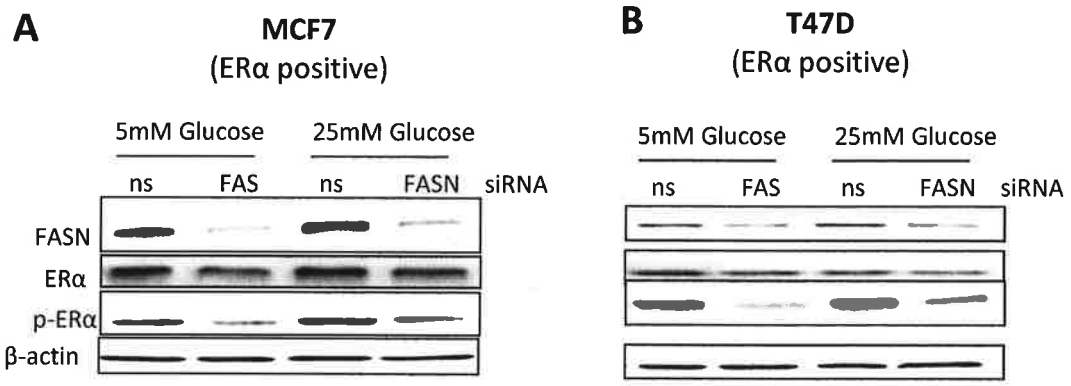
A
MCF7
(ERα positive)
5mM Glucose
25mM Glucose
ns
FAS
ns
FASN
siRNA
FASN
ERα
p-ERα
β-actin
B
T47D
(ERα positive)
5mM Glucose
25mM Glucose
ns
FAS
ns
FASN
siRNA

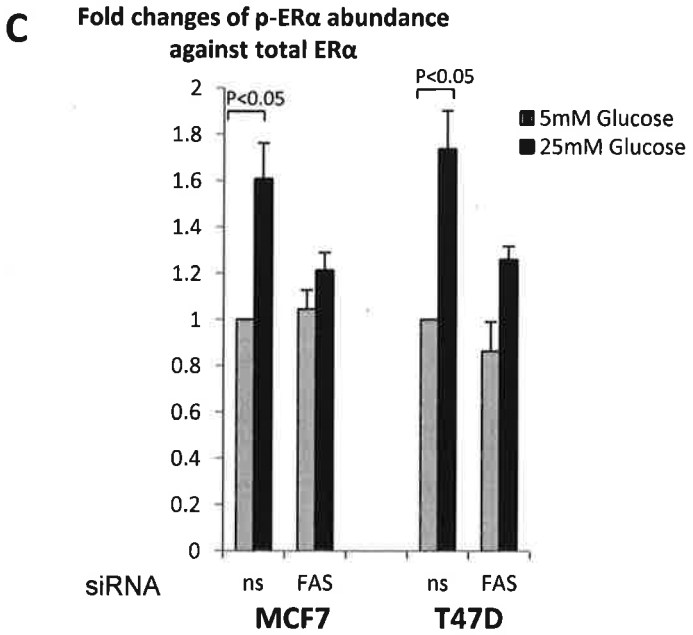
C
Fold changes of p-ERα abundance against total ERα
P<0.05
P<0.05
5mM Glucose
25mM Glucose
2
1.8
1.6
1.4
1.2
1
0.8
0.6
0.4
0.2
0
siRNA
ns
FAS
ns
FAS
MCF7
T47D

Figure 5

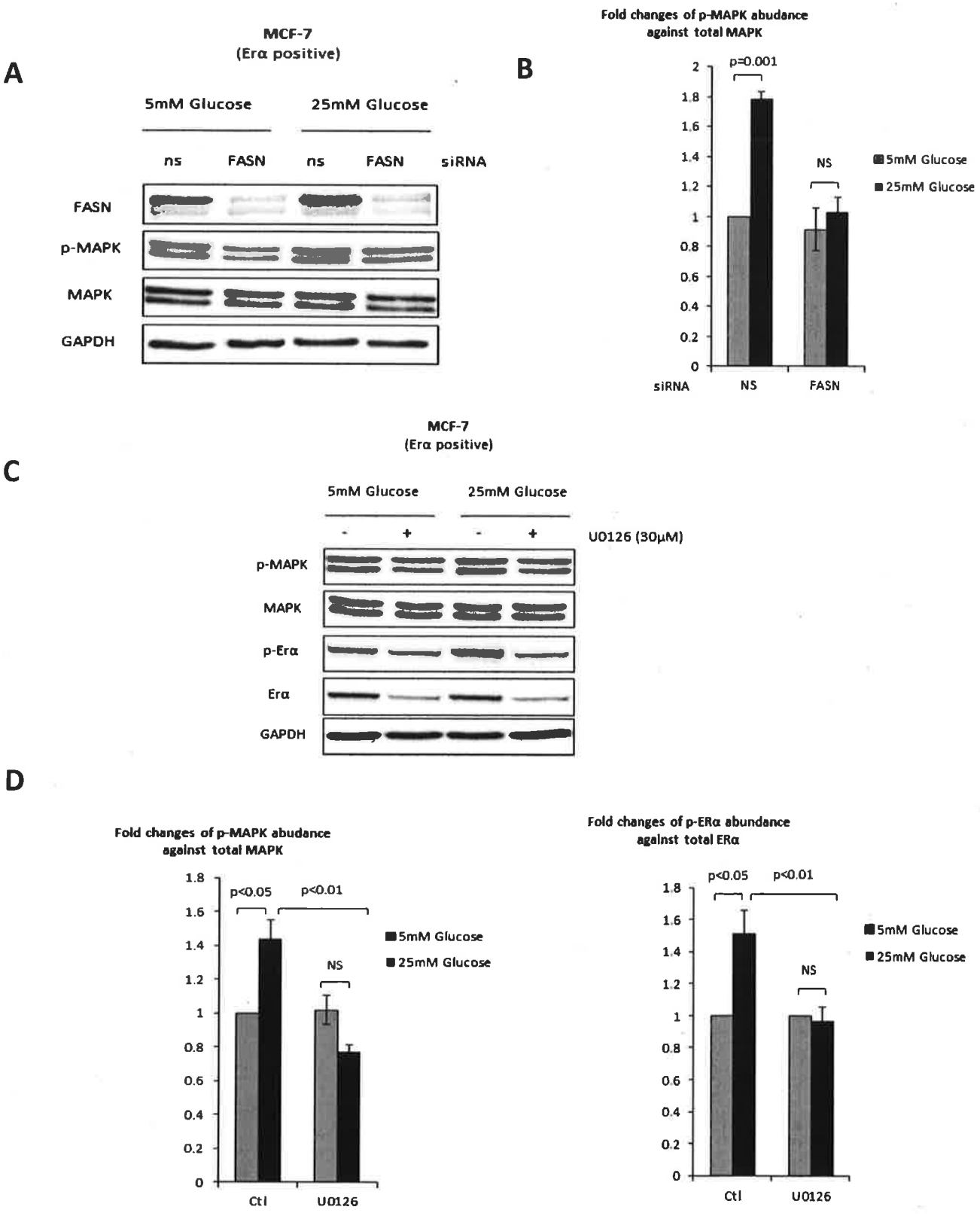
A
MCF-7
(Erα positive)
5mM Glucose
25mM Glucose
ns
FASN
ns
FASN
siRNA
FASN
p-MAPK
MAPK
GAPDH
B
Fold changes of p-MAPK abudance against total MAPK
p=0.001
NS
5mM Glucose
25mM Glucose
siRNA
NS
FASN
C
MCF-7
(Erα positive)
5mM Glucose
25mM Glucose
-
+
-
+
U0126 (30μM)
p-MAPK
MAPK
p-Erα
Erα
GAPDH
D
Fold changes of p-MAPK abudance against total MAPK
p<0.05
p<0.01
NS
5mM Glucose
25mM Glucose
Ctl
U0126
Fold changes of p-ERα abundance against total ERα
p<0.05
p<0.01
NS
5mM Glucose
25mM Glucose
Ctl
U0126

Figure 6

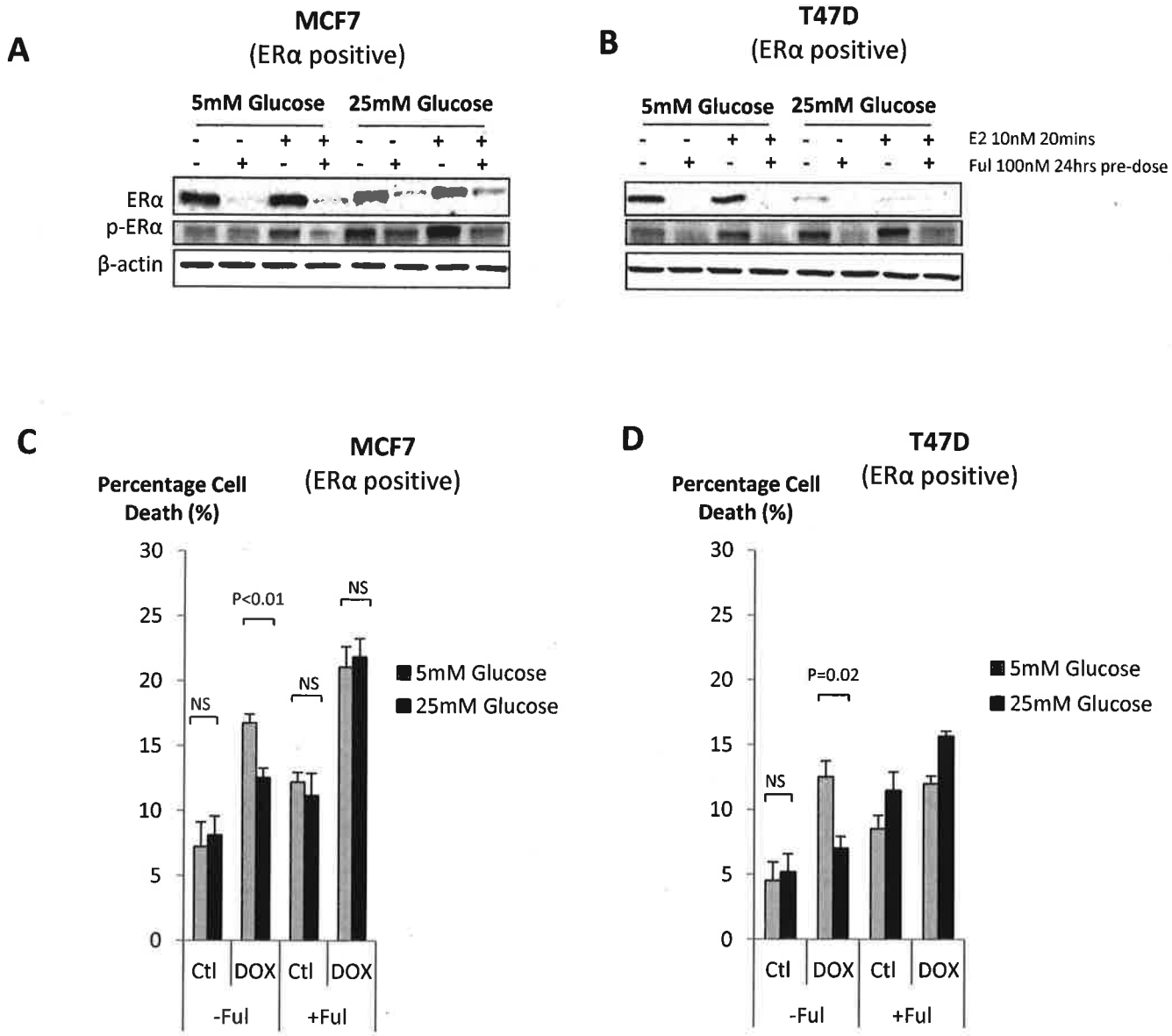
A
MCF7
(ERα positive)
5mM Glucose
25mM Glucose
ERα
p-ERα
β-actin
B
T47D
(ERα positive)
5mM Glucose
25mM Glucose
E2 10nM 20mins
Ful 100nM 24hrs pre-dose
C
MCF7
(ERα positive)
Percentage Cell Death (%)
P<0.01
NS
NS
NS
5mM Glucose
25mM Glucose
Ctl
DOX
Ctl
DOX
-Ful
+Ful
D
T47D
(ERα positive)
Percentage Cell Death (%)
P=0.02
NS
5mM Glucose
25mM Glucose
Ctl
DOX
Ctl
DOX
-Ful
+Ful

Figure 7

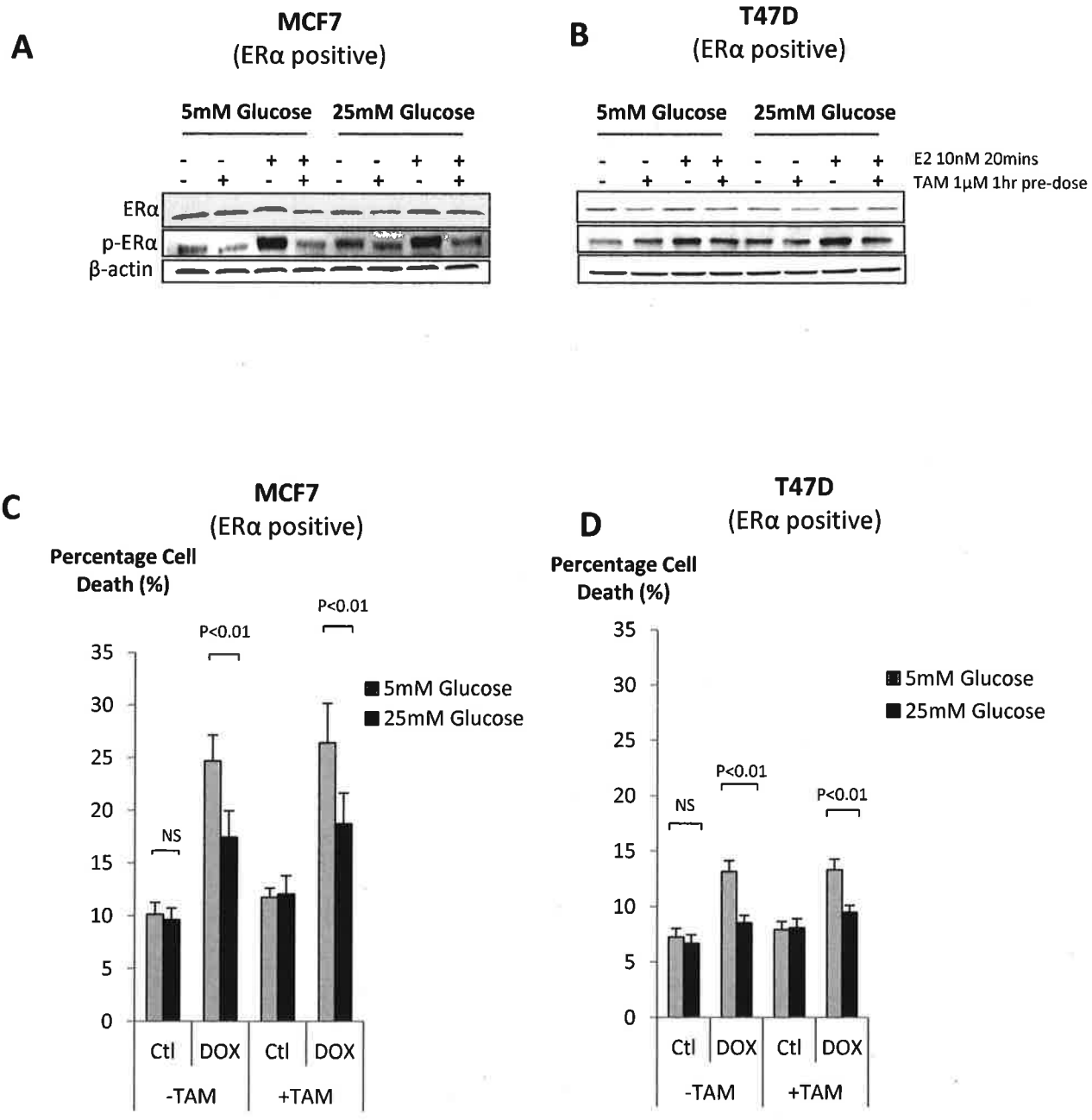
A
MCF7
(ERα positive)
5mM Glucose
25mM Glucose
ERα
p-ERα
β-actin
B
T47D
(ERα positive)
5mM Glucose
25mM Glucose
E2 10nM 20mins
TAM 1μM 1hr pre-dose
C
MCF7
(ERα positive)
Percentage Cell Death (%)
P<0.01
P<0.01
NS
5mM Glucose
25mM Glucose
Ctl
DOX
Ctl
DOX
-TAM
+TAM
D
T47D
(ERα positive)
Percentage Cell Death (%)
NS
P<0.01
P<0.01
5mM Glucose
25mM Glucose
Ctl
DOX
Ctl
DOX
-TAM
+TAM

Supplementary Figure 1

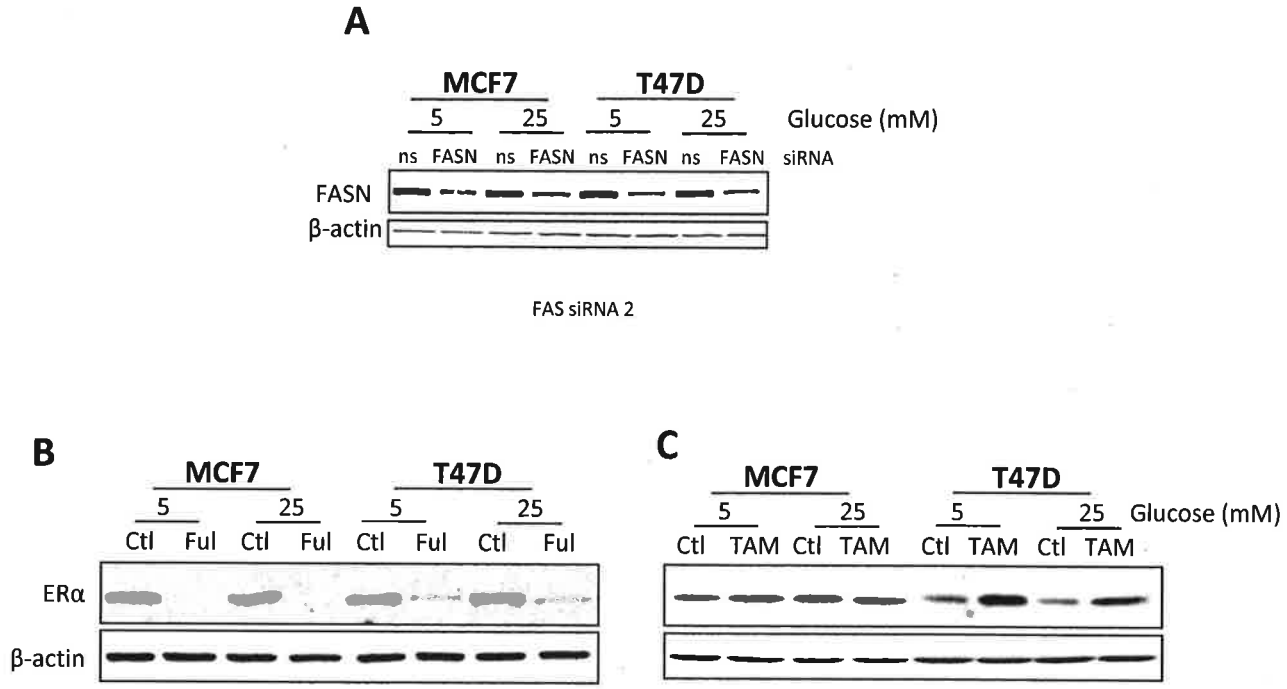

Supplementary Figure 2

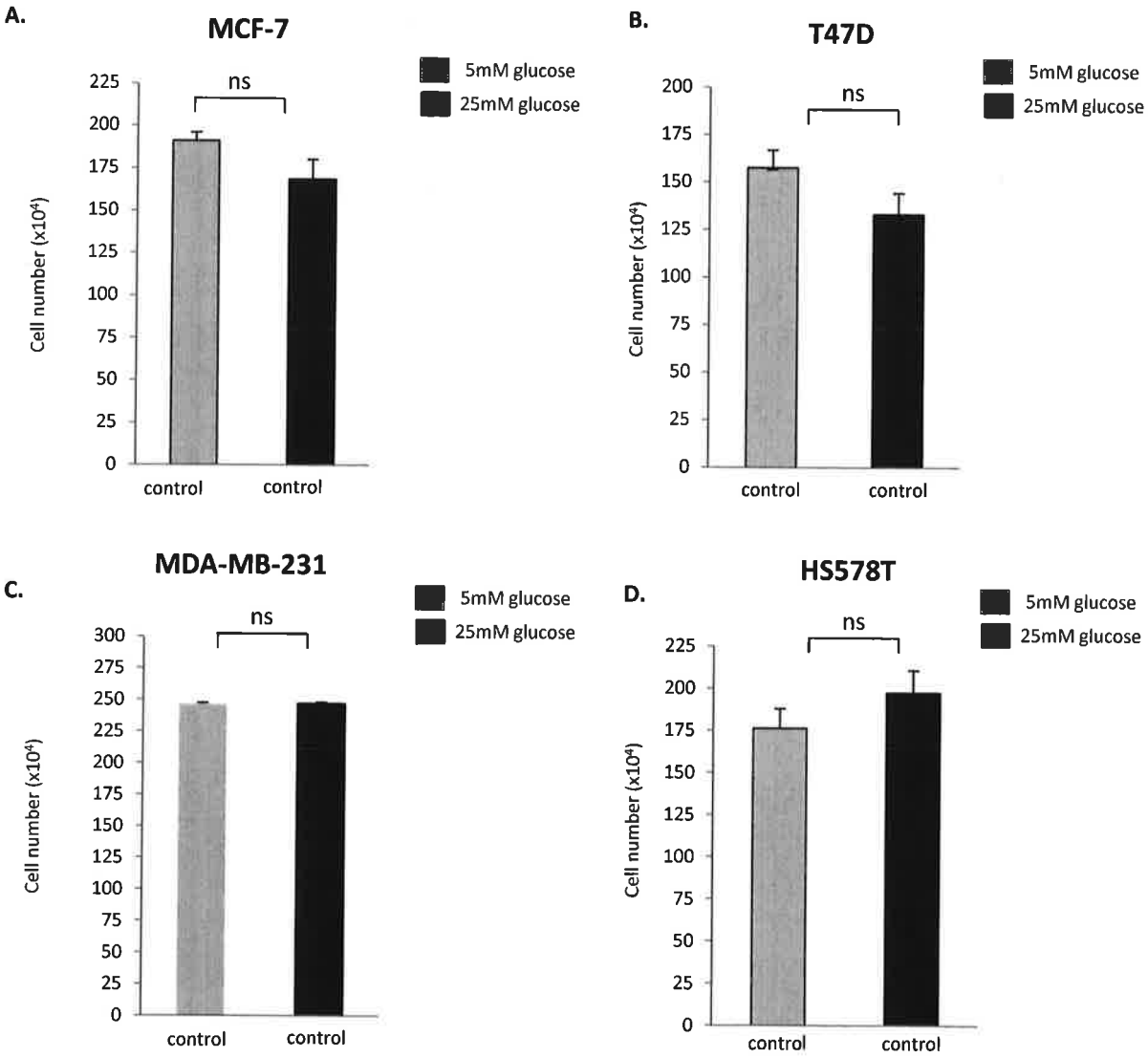

Supplementary Figure 3

A

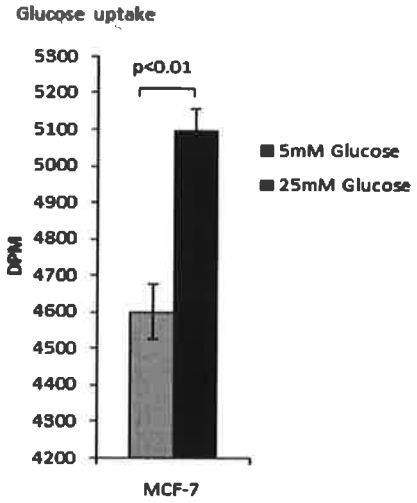

B

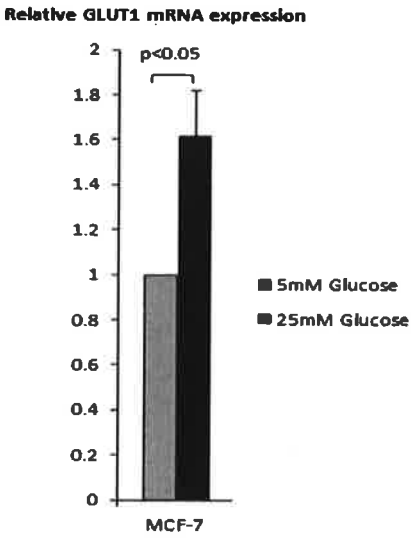

C